Article

Photochromism of *Anabaena* Sensory Rhodopsin

Akira Kawanabe, Yuji Furutani, Kwang-Hwan Jung, and Hideki Kandori

J. Am. Chem. Soc., **2007**, 129 (27), 8644-8649• DOI: 10.1021/ja072085a • Publication Date (Web): 15 June 2007

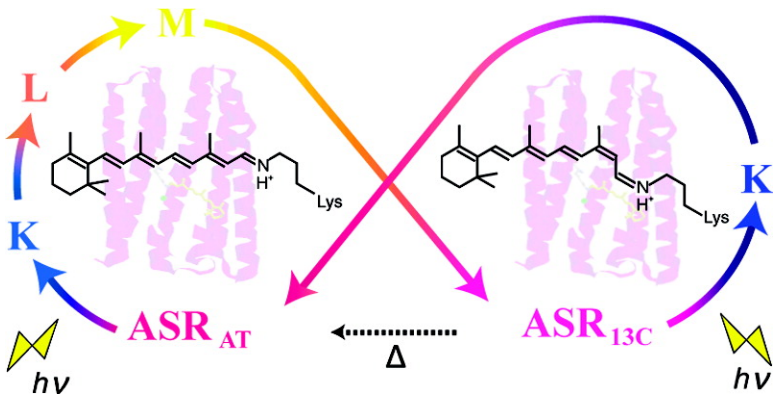

More About This Article

Additional resources and features associated with this article are available within the HTML version:

- Supporting Information
- Links to the 1 articles that cite this article, as of the time of this article download
- Access to high resolution figures
- Links to articles and content related to this article
- Copyright permission to reproduce figures and/or text from this article

View the Full Text HTML

J|A|C|S
ARTICLES
Published on Web 06/15/2007

Photochromism of *Anabaena* Sensory Rhodopsin

Akira Kawanabe,[‡] Yuji Furutani,[‡] Kwang-Hwan Jung,[⊥] and Hideki Kandori*,[‡]

Contribution from the Department of Materials Science and Engineering, Nagoya Institute of Technology, Showa-ku, Nagoya 466-8555, Japan, and Department of Life Science and Interdisciplinary Program of Integrated Biotechnology, Sogang University, Shinsu-Dong 1, Mapo-Gu, Seoul 121-742, Korea

Received March 24, 2007; E-mail: kandori@nitech.ac.jp

Abstract: Protein-controlled photochemical reactions often mediate biological light-signal and light-energy conversions. Microbial rhodopsins possess all-*trans* or 13-*cis* retinal as the chromophore in the dark, and in the light-driven proton pump, bacteriorhodopsin (BR), the stable photoproduct at the end of the functional cycle of the all-*trans* form is 100% all-*trans*. In contrast, a microbial rhodopsin discovered in *Anabaena* PCC7120 is believed to function as a photochromic sensor. For *Anabaena* sensory rhodopsin (ASR), the photoreaction is expected to be not cyclic, but photochromic. The present low-temperature UV−visible spectroscopy of ASR indeed revealed that the stable photoproduct of the all-*trans* form in ASR is 100% 13-*cis*, and that of the 13-*cis* form is 100% all-*trans*. The complete photocycle for the proton pump in BR and the complete photochromism for the chromatic sensor of ASR are highly advantageous for their functions. Thus, the microbial rhodopsins have acquired unique photoreactions, in spite of their similar structures, during evolution.

1. Introduction

Rhodopsins convert light into signal or energy, and retinal is their chromophore molecule.[1−3] The retinal forms a mostly protonated Schiff base linkage (C═NH$^+$) with a lysine at the seventh helix. It is well-known that the protein environment of rhodopsins accommodates the retinal chromophore optimally for its functions. For example, the specific chromophore−protein interaction leads to wide color tuning in human visual pigments with a common chromophore (11-*cis* retinal),[4] and protein controls the highly efficient photoisomerization from 11-*cis* to the all-*trans* form in visual rhodopsins.[5] Specific control of retinal photochemistry by protein can be also seen in rhodopsins from halophilic archaebacteria such as the light-driven proton pump bacteriorhodopsin (BR).[5−7] Unlike visual rhodopsins, BR accommodates the retinal chromophore as the all-*trans*,15-*anti* (AT; BR_{AT}) and 13-*cis*,15-*syn* (13C; BR_{13C}) forms (Figure 1A).[8] BR_{AT} and BR_{13C} are in equilibrium in the dark, while only BR_{AT} possesses proton-pump activity (Figure 1B). Absorption of light by BR_{AT} yields isomerization to the 13-*cis*,15-*anti* form, which triggers a cyclic reaction that comprises the series of intermediates, K, L, M, N, and O.[6,7] During the photocycle, one proton is translocated from the cytoplasmic to extracellualr side.

Photoexcitation of BR_{13C} partially converts it to BR_{AT}, which is called "light-adaptation", but BR_{AT} is not converted into BR_{13C} photochemically. Photocycle of BR_{AT} with 100% yield is advantageous for repeating the proton-pumping cycle. This is also the case for other proton pumps found in eubacteria (proteorhodopsin)[9] and eucaryotes (*Leptosphaeria* rhodopsin).[10] In addition, haloarchaeal sensory rhodopsins possess only the AT chromophore in the dark, indicating that its photocycle is important also for light-signal conversion.[11,12] Thus, the photocycle of the AT form with 100% yield has been the common mechanism for the functional processes of microbial rhodopsins.

Recently, a microbial rhodopsin has been discovered in *Anabaena* (Nostoc) PCC7120, which is believed to function as a photoreceptor for chromatic adaptation.[13] In fact, the expected photochromism was found between the AT and 13C forms for *Anabaena* sensory rhodopsin (ASR).[14] These findings imply strongly branching reactions, from ASR_{AT} to ASR_{13C} and from ASR_{13C} to ASR_{AT} (Figure 1C), in striking contrast to what is known for microbial rhodopsins. Ideally, the conversion ratios should be unity for photochromic reactions ($x = y = 1$ in Figure

[‡] Nagoya Institute of Technology.
[⊥] Sogang University.

(1) Birge, R. R. *Biochim. Biophys. Acta* **1990**, *1016*, 293−327.
(2) Spudich, J. L.; Yang, C. S.; Jung, K. H.; Spudich, E. N. *Annu. Rev. Cell. Dev. Biol.* **2000**, *16*, 365−392.
(3) Kandori, H. *Retinal Binding Proteins: From cis-trans Isomerization in Biochemistry*; Wiley-VCH: Freiburg), 2006; Chapter 4.
(4) Kochendoerfer, G. G.; Lin, S. W.; Sakmar, T. P.; Mathies, R. *Trends. Biochem. Sci.* **1999**, *24*, 300−305.
(5) Kandori, H.; Shichida, Y.; Yoshizawa, T. *Biochemistry (Moscow)* **2001**, *66*, 1197−1209.
(6) Haupts, U.; Tittor, J.; Oesterhelt, D. *Annu. Rev. Biophys. Biomol. Struct.* **1999**, *28*, 367−399.
(7) Lanyi, J. K. *J. Phys. Chem. B* **2000**, *104*, 11441−11448.
(8) Scherrer, P.; Mathew, M. K.; Sperling, W.; Stoecknius, W. *Biochemistry* **1989**, *28*, 829−834.
(9) Beja, O.; Aravind, L.; Koonin, E. V.; Suzuki, M. T.; Hadd, A.; Nguyen, L. P.; Jovanovich, S. B.; Gates, C. M.; Feldman, R. A.; Spudich, J. L.; Spudich, E. N.; Delong, E. F. *Science* **2000**, *289*, 1902−1906.
(10) Waschuk, S. K.; Bezerra, A. G., Jr.; Shi, L.; Brown, L. S. *Proc. Natl. Acad. Sci. U.S.A.* **2005**, *102*, 6879−6883.
(11) Imamoto, Y.; Shichida, Y.; Hirayama, J.; Tomioka, H.; Kamo, N.; Yoshizawa, T. *Biochemistry* **1992**, *31*, 2523−2528.
(12) Tsuda, M.; Nelson, B.; Chang, C. H.; Govindjee, R.; Ebrey, T. G. *Biophys. J.* **1985**, *47*, 721−724.
(13) Jung, K. H.; Trivedi, V. D.; Spudich, J. L. *Mol. Microbiol.* **2003**, *47*, 1513−1522.
(14) Sineshchekov, O. A.; Trivedi, V. D.; Sasaki, J.; Spudich, J. L. *J. Biol. Chem.* **2005**, *280*, 14663−14668.

10.1021/ja072085a CCC: $37.00

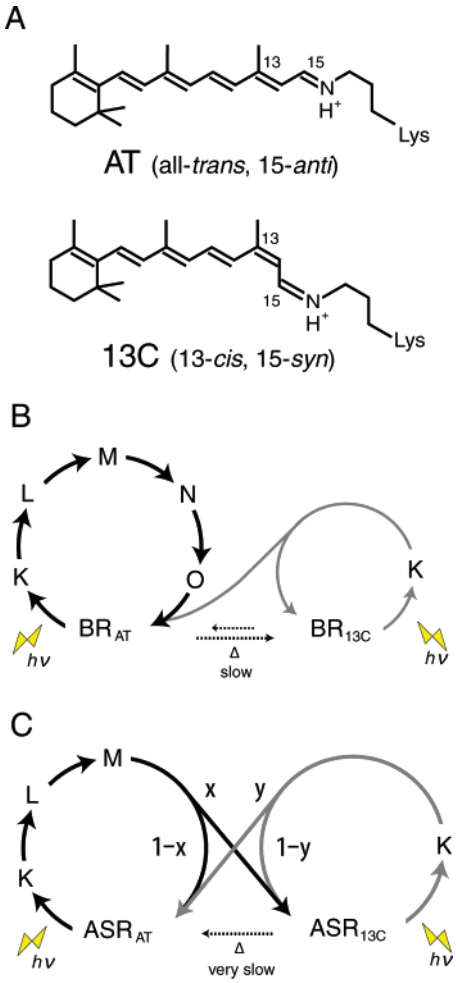

Figure 1. (A) Structure of the retinal chromophore of microbial rhodopsins in the dark. (B) Photo- and thermal reaction scheme in a light-driven proton pump bacteriorhodopsin (BR). Only BR_{AT} possesses proton-pump activity, and the reaction of BR_{AT} is 100% cyclic without any branching reaction into BR_{13C}. Dotted arrows represent the thermal reaction in the dark, where BR_{13C} is more stabilized than BR_{AT}. (C) Photo- and thermal reaction scheme in *Anabaena* sensory rhodopsin (ASR). While ASR_{AT} is a predominant species in the dark (dotted arrow), photoexcitation of ASR_{AT} and ASR_{13C} yields the reaction of each species, either cyclic or branching, leading to the photocycle or photochromism, respectively. *x* and *y* are the branching ratios from ASR_{AT} and ASR_{13C}, respectively.

1C), but this is exactly the opposite of the properties of pump rhodopsins, such as BR. X-ray crystal structures reported similar chromophore structures and protein environments for ASR_{AT}[15] and BR_{AT}.[16] Do photochromic reactions indeed take place for ASR_{AT} and ASR_{13C}? In this paper, we determined the branching ratios (*x* and *y* values) for ASR_{AT} and ASR_{13C} by means of low-temperature UV−visible spectroscopy. Surprisingly, the obtained *x* and *y* values were unity, indicating that the photoreactions of ASR_{AT} and ASR_{13C} are completely photochromic. The complete photochromic reactions are highly advantageous for the chromatic sensor function of ASR.

2. Materials and Methods

The ASR protein with a histidine tag at the C-terminus was expressed in *Escherichia coli*, solubilized with 1.0% *n*-dodecyl-β-D-maltoside, and purified by a Ni^{2+}-column.[17,18] The purified ASR sample was then reconstituted into L-α-phosphatidylcholine (PC) liposomes by the removal of the detergent with Bio-beads, where the molar ratio of the added PC to ASR was 50:1. The ASR protein in PC liposomes was washed three times with a buffer [2 mM sodium phosphate (pH 7.0)]. A 60-μL aliquot was deposited on a BaF_2 window of 18-mm diameter and dried in a glass vessel with evaporation by an aspirator.

The fully hydrated ASR film sample was used for low-temperature UV−visible spectroscopy, where three to five independent measurements were averaged. The UV−visible spectra were measured by a UV−visible spectrometer (V-550, JASCO) equipped with a cryostat (OptistatDN, Oxford). The cryostat was equipped with a temperature controller (ITC-4, Oxford), and the temperature was regulated with 0.1 K precision. A previous HPLC study showed that the completely dark-adapted ASR in PC liposomes is in the all-*trans* form predominantly (97.1 ± 0.1%).[18] On the other hand, illumination of ASR with >560-nm light (O-58 cutoff filter, Toshiba) from a 1-kW halogen−tungsten lamp for 1 min at 277 K yields formation of 77.9(±1.7)% 13-*cis* form.[18]

3. Results and Discussion

3.1. Photoconversion of ASR_{AT} (1) Photoreaction at 170 K. We first examined the branching ratio of ASR_{AT} (*x* value in Figure 1C) because previous HPLC analysis revealed that the dark-adapted ASR in PC liposomes contains predominantly (97%) ASR_{AT}.[18] Dark-adapted ASR was illuminated at 170 K, and then warmed to 277 K. The photoconversion yield of ASR_{AT} to its intermediates was calculated using the spectra at 170 K, which was compared with the conversion of ASR_{AT} to ASR_{13C} at 277 K. The black line in Figure 2A shows the absorption spectrum of the dark-adapted ASR at 170 K (λ_{max} = 554 nm). Illumination at >580 nm (red line) or 501 nm (blue line) resulted in reduction of the peak absorbance and increase of the shorter or longer wavelength tail, indicating the formation of the L and K photointermediates, respectively. Figure 2B shows the corresponding difference spectra, and positive peaks at 474 and 605 nm are characteristic absorption of the L and K intermediates, respectively. On the other hand, no positive band at about 400 nm indicates that the M intermediate is not formed at 170 K.

Since the red and blue spectra in Figure 2B contain contribution of the L and K intermediates, we next obtained the K minus ASR_{AT} and L minus ASR_{AT} spectra. The L minus ASR_{AT} spectrum was obtained by subtracting the blue spectrum from the red one in Figure 2B, so that the spectral shape at about 600 nm coincides with that of the absolute spectrum of the dark-adapted ASR (black line in Figure 2A). The red spectrum in Figure 2C represents the L minus ASR_{AT} spectrum thus obtained. Then, the L minus ASR_{AT} spectrum was subtracted from the blue spectrum in Figure 2B so as to resemble that at 130 K (black dotted line in Figure 2C), where the photoproduct is only the K intermediate. The blue spectrum in Figure 2C represents the resulting K minus ASR_{AT} spectrum. Isosbestic points are at 520 nm between ASR_{AT} and L, and at 575 nm between ASR_{AT} and K.

We then determined the absorption spectra of the K and L intermediates of ASR_{AT} at 170 K. Absorption spectra of intermediates can be obtained from the difference spectrum and photoconversion ratio from ASR_{AT} to the intermediate. Five

(15) Vogeley, L.; Sineshchekov, O. A.; Trevedi, V. D.; Sasaki, J.; Spudich, J. L.; Luecke, H. *Science* **2004**, *306*, 1390−1393.
(16) Luecke, H.; Schobert, B.; Richter, H. T.; Cartailler, J. P.; Lanyi, J. K. *J. Mol. Biol.* **1999**, *291*, 899−911.
(17) Furutani, Y.; Kawanabe, A.; Jung, K. H.; Kandori, H. *Biochemistry* **2005**, *44*, 12287−12296.
(18) Kawanabe, A.; Furutani, Y.; Jung, K. H.; Kandori, H. *Biochemistry* **2006**, *45*, 4362−4370.

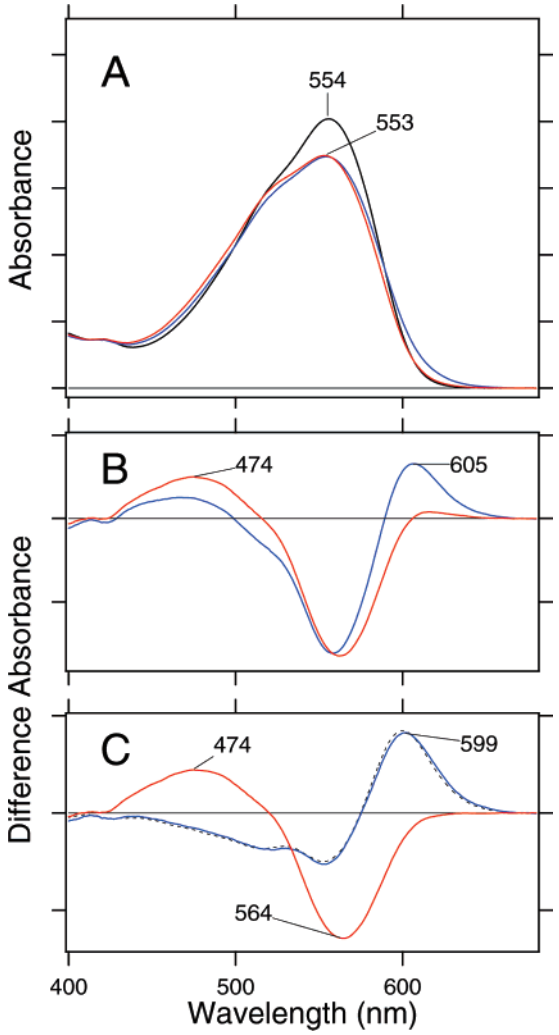

Figure 2. (A) Absorption spectra of the dark-adapted ASR (black line), and illuminated ASR with >580 nm (red line) and 501 nm (blue line) light at 170 K. It should be noted that the dark-adapted ASR corresponds to ASR_{AT}, because it contains negligible amount of ASR_{13C} (2.9%) in the present sample conditions.[18] (B) Light-minus-dark difference absorption spectra of ASR with >580 nm (red line) and 501 nm (blue line) light at 170 K. (C) L minus ASR_{AT} (red line) and K minus ASR_{AT} (blue line) difference absorption spectra at 170 K. Broken black line corresponds to the K minus ASR_{AT} spectrum at 130 K, where only the K intermediate is formed. See text for details.

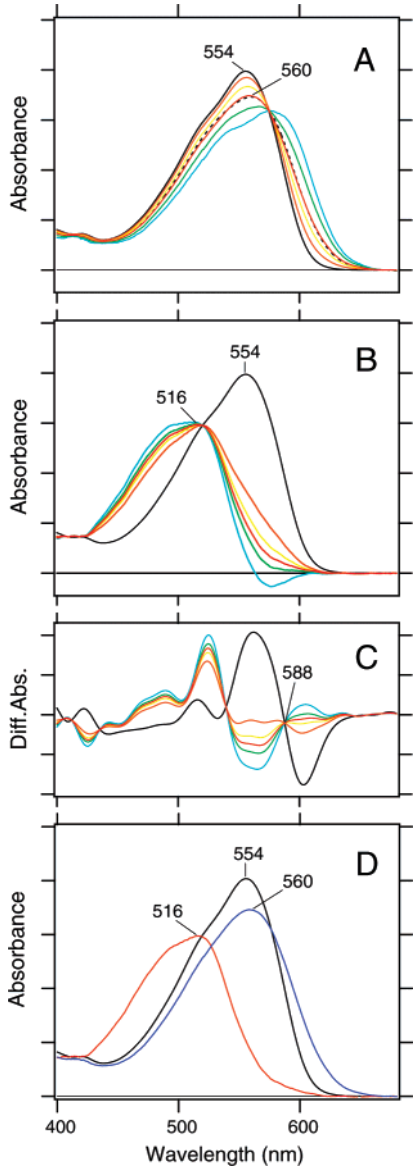

Figure 3. Determination of the absorption spectra of the K and L intermediates of ASR_{AT} at 170 K. (A) Solid black line represents the absorption spectrum of ASR_{AT} at 170 K. The absorption spectrum of the K intermediate can be obtained from the K minus ASR_{AT} difference spectrum (blue line in Figure 2C) and photoconversion ratio from ASR_{AT} to the K intermediate. Five colored lines correspond to the calculated spectra of the K intermediate of ASR_{AT} at various % of conversion (100−17% from orange to blue; 32% for the red line). The broken black line represents the absorption spectrum of the K intermediate of ASR_{AT} at 130 K, which was determined by the method described in Figure S1. Since the red spectrum coincides well with the broken black line, we regarded the red one as the absorption spectrum of the K intermediate of ASR_{AT} at 170 K. (B) The solid black line represents absorption spectrum of ASR_{AT} at 170 K. The absorption spectrum of the L intermediate can be obtained from the L minus ASR_{AT} difference spectrum (red line in Figure 2C) and photoconversion ratio from ASR_{AT} to the L intermediate. Five colored lines correspond to the calculated spectra of the L intermediate of ASR_{AT} at various percentages of conversion (18−12% from orange to blue; 14% for the red line). (C) Second derivatives of absorption spectra in Figure 3B, where the corresponding spectra are shown by the same color. The second derivative of the ASR_{AT} spectrum (black line) coincides with the zero line at 588 nm. We assume that the L intermediate does not contain a spectral component in the second derivative at >588 nm. Consequently, we regard the red one in Figure 3B as the absorption spectrum of the L intermediate of ASR_{AT} at 170 K. (D) Absorption spectra of ASR_{AT} (black line), the K intermediate (blue line), and the L intermediate (red line) at 170 K. The spectra of the K and L intermediates are reproduced from the red spectra in Figure 3A and B, respectively.

colored lines in Figure 3A or B correspond to the calculated spectra of the K intermediate of ASR_{AT} or the L intermediate of ASR_{AT} at various percentages of conversion, respectively. The broken black line in Figure 3A represents the absorption spectrum of the K intermediate of ASR_{AT} at 130 K, which was determined by illuminating ASR_{AT} at two wavelengths as described in Figure S1. We regarded the red spectrum in Figure 3A as the absorption spectrum of the K intermediate of ASR_{AT} at 170 K because the red one coincides well with the broken black line. On the other hand, the absorption spectrum of the L intermediate was determined from the spectral analysis of the second derivatives of the absorption spectra in Figure 3B. The second derivatives in Figure 3C show that the red spectrum coincides with the zero line at >588 nm. On the assumption that the L intermediate does not contain a spectral component in the second derivative at >588 nm, we regarded the red one in Figure 3B as the absorption spectrum of the L intermediate of ASR_{AT} at 170 K. Blue and red spectra in Figure 3D

correspond to the absolute spectra of the K and L intermediates, respectively.

3.2. Photoconversion of ASR_{AT} (2) Thermal Relaxation by Warming the Sample from 170 to 277 K. We reconstituted the experimentally obtained spectra (dotted black lines in Figure 4A and C) by use of the spectra in Figure 3D. For the illumination at >580 nm, the dotted black spectrum in Figure 4A is well coincident with the sum of 78% ASR, 5% K, and 17% L (green line in Figure 4A), indicating the 22(±2)% conversion to intermediates at 170 K. On the other hand, for the illumination at 501 nm, the dotted black spectrum in Figure 4C is well coincident with the sum of 68% ASR, 18% K, and 14% L (green line in Figure 4C), indicating the 32(±5)% conversion at 170 K.

We then warmed these states from 170 to 277 K so as to complete the thermal reactions of the K and L states to their end products, and calculated the conversion yield from the spectra. Dotted black lines in Figure 4B and D represent the spectra at 277 K after illumination at >580 and 501 nm, respectively, at 170 K. By the use of the absorption spectra of ASR_{AT} and ASR_{13C}, the percentage of conversions were calculated to be 23(±2)% and 34(±4)% in Figure 4B and D, respectively. The branching ratios (*x* in Figure 1) were thus determined to be 1.02 ± 0.13 and 1.10 ± 0.09 for illuminations at >580 and 501 nm, respectively. These values demonstrate that the K and L intermediates formed from ASR_{AT} are completely converted into ASR_{13C} without regaining the initial state in a photocyclic reaction.

By means of low-temperature FTIR spectroscopy, we had previously suggested that the primary photoproduct of ASR_{AT} is the 13-*cis*,15-*anti* form as in BR (Figure 5).[17] In BR, thermal isomerization takes place at the C13═C14 bond with virtually 100% yield, recovering the original AT state. In contrast, in ASR thermal isomerization is likely to occur at the C15═N bond following photoisomerization of ASR_{AT}, which converts to the 13C state with 100% yield (Figure 5).

3.3. Photoconversion of ASR_{13C} (1) Relative Photoconversion Yields of ASR_{AT} and ASR_{13C} at 277 K. What is the branching ratio (*y* value in Figure 1C) from ASR_{13C}? Unlike ASR_{AT} that is present as nearly the only state in dark-adapted ASR, ASR_{13C} is present in a mixture with ASR_{AT}. Therefore, we attempted to determine the branching ratio on the basis of relative photoconversion yields. A previous study showed that the dark-adapted or light-adapted ASRs in PC liposomes possess 97.1% ASR_{AT} and 2.9% ASR_{13C} or 22.1% ASR_{AT} and 77.9% ASR_{13C}, respectively.[18] Since ASR_{AT} has greater extinction than ASR_{13C} at 500−600 nm (Figure 4B and D), illumination of the dark-adapted ASR yields an absorption decrease in this wavelength region. In contrast, illumination of light-adapted ASR results in the increase of absorption at 500−600 nm, as reported previously.[15] The isosbestic point of ASR_{AT} and ASR_{13C} is located at 496 nm (Figure 4B and D).

In Figure 6, we illuminated the dark-adapted and light-adapted ASR with a 496-nm light at 277 K, and the changes in absorbance at 569 nm (difference absorption maximum between ASR_{AT} and ASR_{13C} at 277 K) were plotted as the function of illumination time. Thermal conversion from ASR_{13C} to ASR_{AT} is negligible, because it takes 90 min ($\tau_{1/2}$) for ASR in PC liposomes at 277 K (data not shown). Absorbance at 569 nm decreases and increases for the dark-adapted and light-adapted

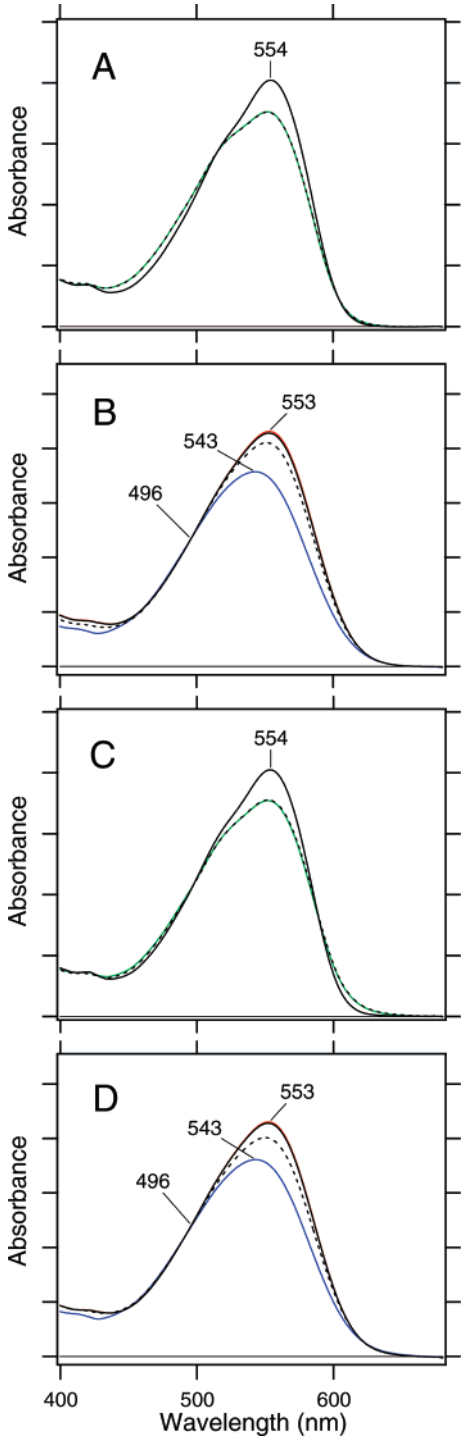

Figure 4. (A and C) Absorption spectra of the dark-adapted ASR before (solid black lines) and after (dotted black lines) illuminations with >580 nm (A) and 501 nm (C) lights at 170 K. Green lines represent the reconstituted spectra by use of those in Figure 2D. Under the present illumination conditions, 22(±2)% and 32(±5)% portions were converted into the intermediates in A and C, respectively. (B and D) Solid black lines represent absorption spectra of the dark-adapted ASR at 277 K. Red and blue lines correspond to the calculated absorption spectra of ASR_{AT} and ASR_{13C} at 277 K, respectively, which were obtained from those of dark- and light-adapted ASR and the HPLC analysis.[18] Dotted black lines represent absorption spectra at 277 K after illuminations with >580 nm (B) and 501 nm (D) lights at 170 K. Under the present illumination conditions, 23-(±2)% and 34(±4)% portions were converted from ASR_{AT} to ASR_{13C} at 277 K in b and d, respectively. From a−d, the branching ratio (*x* in Figure 1C) is 1.02 ± 0.13 and 1.10 ± 0.09 for illuminations at >580 and 501 nm, respectively, indicating complete branching reactions from ASR_{AT} for both illumination conditions.

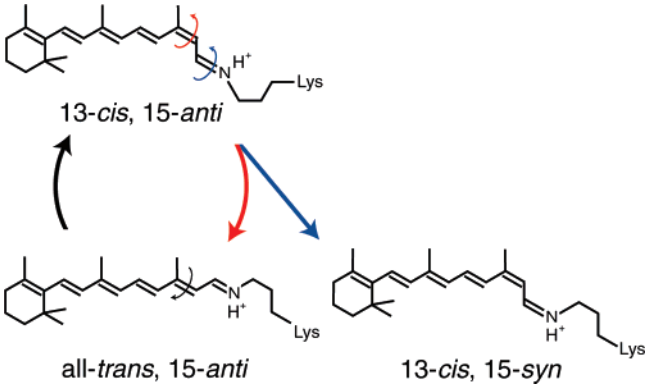

Figure 5. Structural changes of the all-*trans*,15-*anti* chromophore during photoreactions. The all-*trans*,15-*anti* form, either in BR_{AT} or ASR_{AT}, is first photoconverted to the 13-*cis*,15-*anti* form, followed by thermal isomerization at C13═C14 or C15═N position in BR or ASR, respectively. Such thermal relaxations led to 100% photocyclic and photochromic reactions for BR_{AT} and ASR_{AT}, respectively.

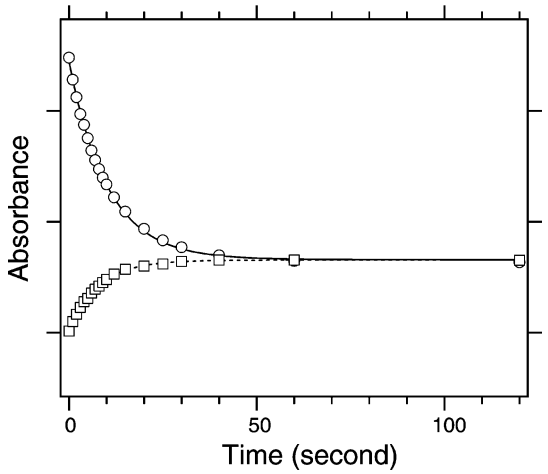

Figure 6. Absorption changes at 569 nm of the dark-adapted (open circles) and light-adapted (open triangles) ASR after illumination at the isosbestic point of ASR_{AT} and ASR_{13C} (496 nm) at 277 K. Absorption changes were fitted by single exponentials (solid and broken lines), and the ratio of the initial slope (light-adapted ASR/dark-adapted ASR) was 0.40:1. By taking into account the contents of ASR_{AT} and ASR_{13C} in each state, the ratio between ASR_{13C}-to-ASR_{AT} and ASR_{AT}-to-ASR_{13C} was determined to be 0.77 (±0.04).

ASR, respectively, and both curves eventually coincide after long illumination (Figure 6). The time courses are well fitted by single exponentials, and each photoconversion yield can be obtained from the initial slope ($t = 0$). By taking into account the contents of ASR_{AT} and ASR_{13C} in the dark-adapted and light-adapted forms, we determined the ratio between ASR_{13C}-to-ASR_{AT} and ASR_{AT}-to-ASR_{13C} to be 0.77 (±0.04):1. [Sineshchekov et al. estimated a similar photoconversion yield to be 0.3:1 from the HPLC analysis of the photosteady state mixture with white or >520-nm light illumination.[14] While the accurate photoconversion yield is determined by the present method (from the initial slope after illumination at their isosbestic point), such a big difference (0.77-times vs 0.3-times) should be explained. We confirmed that the spectral analysis of the photosteady state, not initial slope, in Figure 6 yields the ratio to be similar (0.75:1). On the other hand, the ratio between ASR_{13C}-to-ASR_{AT} and ASR_{AT}-to-ASR_{13C} was significantly reduced by illumination at longer wavelengths, which is close to the value reported by Sineshchekov et al.[14] Thus, the photoconversion yield depends on the illumination wavelength;

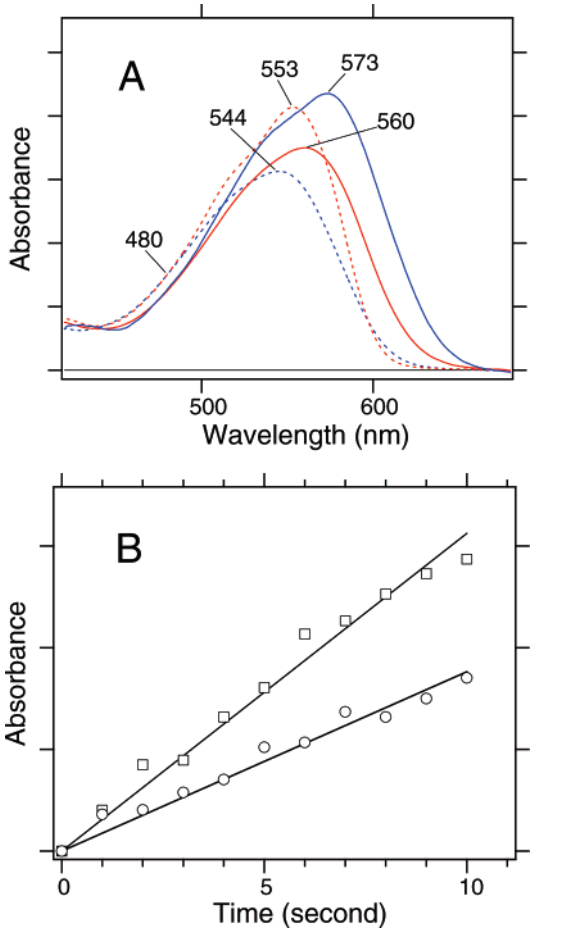

Figure 7. (A) Red and blue broken lines correspond to the absorption spectra of ASR_{AT} and ASR_{13C} at 130 K, respectively, which were obtained from those of the dark- and light-adapted ASR and the HPLC analysis.[18] The isosbestic point is located at 480 nm. Solid red and blue lines represent absorption spectra of the K intermediates of ASR_{AT} and ASR_{13C}, respectively, at 130 K, which were obtained according to the procedure in Figure S1. (B) Time-dependent absorbance changes of the dark-adapted (open circles) and light-adapted (open triangles) ASR. Each sample was illuminated at the isosbestic point at 130 K (480 nm; Figure 7A), and absorbance changes were monitored at 596 and 590 nm for the dark-adapted and light-adapted ASR, respectively.

0.77 by the 496-nm illumination and about 0.3 by the illumination at >520 nm. We infer that under the photostationary conditions at >520 nm, the intermediate state of ASR_{13C} is photoexcited, presumably forming the original ASR_{13C}, while that of ASR_{AT} (the M state) is not. Consequently, ASR_{13C} is accumulated, and the ratio between ASR_{13C}-to-ASR_{AT} and ASR_{AT}-to-ASR_{13C} is apparently lowered.] Since the sample is illuminated at the isosbestic point, the ratio is directly correlated with the relative photoconversion yields. Although this value apparently shows a lower branching ratio for ASR_{13C} than for ASR_{AT} ($x = 1$), it should be noted that the photoisomerization quantum yields are not taken into account in this estimate. A lower photoisomerization quantum yield of ASR_{13C} may provide a lower value for ASR_{13C}, and it was indeed the case.

3.4. Photoconversion of ASR_{13C} (2) Relative Photoisomerization Quantum Yields of ASR_{AT} and ASR_{13C} at 130 K. We next compared the relative quantum yields for the photoisomerization of ASR_{AT} and ASR_{13C} by comparing the formation of their K intermediates at 130 K. Since the molar extinction coefficients of their K intermediates are required for the calculation, we determined the absorption spectra of the K

intermediates of ASR_{AT} and ASR_{13C} according to the procedure in Figure S1. Solid red and blue lines in Figure 7A represent absorption spectra of the K intermediates of ASR_{AT} and ASR_{13C}, respectively. Interestingly, the amplitude of the K state is decreased for ASR_{AT} but increased for ASR_{13C}. Together with the absorption of ASR_{AT} greater than that of ASR_{13C} (broken lines in Figure 7A), this suggests that the 13C *trans* form has a large absorption in the protein pocket of ASR.

We then illuminated the dark-adapted and light-adapted ASR at 480 nm, the isosbestic point of ASR_{AT} and ASR_{13C}, at 130 K (Figure 7A). Figure 7B shows time-dependent absorbance changes at their difference absorption maxima (596 and 590 nm) of the dark-adapted and light-adapted ASR. The increase of absorbance is greater for the light-adapted ASR, which contains more ASR_{13C}, and originates also from the larger absorbance of the K intermediate of ASR_{13C}. By considering the molar extinction coefficients of the K intermediates, the relative quantum yield for the photoisomerization of ASR_{13C} and ASR_{AT} was determined to be 0.73 ($\pm$0.07):1. From the data in Figure 4A and C, the branching ratio of ASR_{13C} (y in Figure 1) was therefore determined to be 1.06 ± 0.11. This value demonstrates that the K intermediate formed from ASR_{13C} is completely converted into ASR_{AT} without regaining the initial state in a photocyclic reaction.

3.5. Functional Optimization of Photoconversions in Rhodopsins. The present results reveal that the branching reactions take place with 100% efficiency, both from ASR_{AT} and ASR_{13C}. Although the present results were obtained for ASR in liposomes, not in native membranes, this characteristic is highly advantageous for a photochromic sensor. On the other hand, the AT form of BR has 100% photocyclic efficiency (Figure 5), which is important for the proton pump. Thus, it is concluded that ASR and BR have been optimized for their functions, presumably during evolution.

It is intriguing that the structures of the chromophore and its binding pocket are similar between ASR[15] and BR,[16] although their amino acid sequences are not highly homologous (60%). Our FTIR study revealed that hydrogen bond of the Schiff base is similarly strong in ASR and BR, and they are similarly cleaved after retinal photoisomerization.[17] Replacement of aspartate (Asp212 of BR) by proline in ASR (Pro206) is one of the structural differences. Another difference is the hydrogen-bonding strength of the water molecule near the Schiff base. BR possesses a strongly hydrogen-bonded water molecule between the Schiff base and its counterion (Asp85), which appears to be a prerequisite for proton-pump function.[19] ASR possesses such a water molecule between the Schiff base and its counterion (Asp75),[15] but its hydrogen bond is much weaker.[17] These small differences may be determinants for distinguishing photocyclic or photochromic reactions. Recently, Sudo and Spudich converted BR into a sensory receptor by mutation of three hydrogen-bonding residues.[20] This finding also suggests that distinct functions are determined by small differences. In addition, the M intermediate is formed during the photoreaction of ASR_{AT} like BR, but Asp75 is not protonated,[21] presumably because the proton is conducted toward the cytoplasmic domain.[22] Further structural analysis of photoreaction intermediates will provide a better understanding of the mechanism for thermal relaxation of the photoisomerized chromophore.

Supporting Information Available: Determination of the absorption spectra of the K intermediates of ASR_{AT} and ASR_{13C} at 130 K. This material is available free of charge via the Internet at http://pubs.acs.org.

JA072085A

(19) Furutani, Y.; Shibata, M.; Kandori, H. *Photochem. Photobiol. Sci.* **2005**, *4*, 661−666.
(20) Sudo, Y.; Spudich, J. L. *Proc. Natl. Acad. Sci. U.S.A.* **2006**, *103*, 16129−16134.
(21) Bergo, V. B.; Ntefidou, M.; Trivedi, V. D.; Amsden, J. J.; Kralj, J. M.; Rothschild, K. J.; Spudich, J. L. *J. Biol. Chem.* **2006**, *281*, 15208−15214.
(22) Shi, L.; Yoon, S. R.; Bezerra, A. G., Jr.; Jung, K. H.; Brown, L. S. *J. Mol. Biol.* **2006**, *358*, 686−700.